Supplemental Information of "Electronic band structure change with structural transition of buckled Au_2X monolayers induced by strain"

Masahiro Fukuda*[a] and Taisuke Ozaki[b]

[1] [a] *Institute for Solid State Physics, The University of Tokyo, 5-1-5 Kashiwanoha, Kashiwa, Chiba 277-8581, Japan. E-mail: masahiro.fukuda@issp.u-tokyo.ac.jp*

[2] [b] *Institute for Solid State Physics, The University of Tokyo, 5-1-5 Kashiwanoha, Kashiwa, Chiba 277-8581, Japan*

S1. SUPPLEMENTAL INFORMATION

In Sec. S1 A, figures and tables about Au_2S are shown. We show the convergence of energy and lattice length for the number of k-mesh and energy cutoff in Table S1 and S2. The Table S3 shows the function types for CB2, CB1, VB1 and VB2. The electronic band structures and DOSs of Au_2S and their decomposed results are shown in Fig. S1 - S3. The Figs. S4 and S5 show molecular orbitals of VB2, VB1, CB1, and CB2 at the Γ point.

In Sec. S1 B, figures and tables about Au_2X (X=S, Se, Te, Si, Ge) and Au_4SSe are shown. The phonon bands are shown in Figs. S6 and S7. The energy curves, electronic band structures, and optical conductivities are shown in Figs. S8 - S11.

A. Au_2S monolayers

TABLE S1: Convergence of energy for the number of k-mesh and energy cutoff $E_{\rm cut}$.

k-mesh	$E_{\rm cut}$ [Ry]	Energy [a.u.]		
		η-Au_2S	θ-Au_2S	$E_\theta - E_\eta$
$5 \times 5 \times 1$	240	-443.3502	-443.3477	0.0026
$7 \times 7 \times 1$	240	-443.3505	-443.3484	0.0021
$5 \times 5 \times 1$	320	-443.3511	-443.3483	0.0028
$7 \times 7 \times 1$	320	-443.3514	-443.3491	0.0023
$9 \times 9 \times 1$	600	-443.3534	-443.3516	0.0018

TABLE S2: Convergence of lattice length for the number of k-mesh and energy cutoff E_{cut}.

k-mesh	E_{cut} [Ry]	Lattice length [Å]	
		η-Au_2S	θ-Au_2S
$5 \times 5 \times 1$	240	5.805	5.610
$9 \times 9 \times 1$	600	5.803	5.605

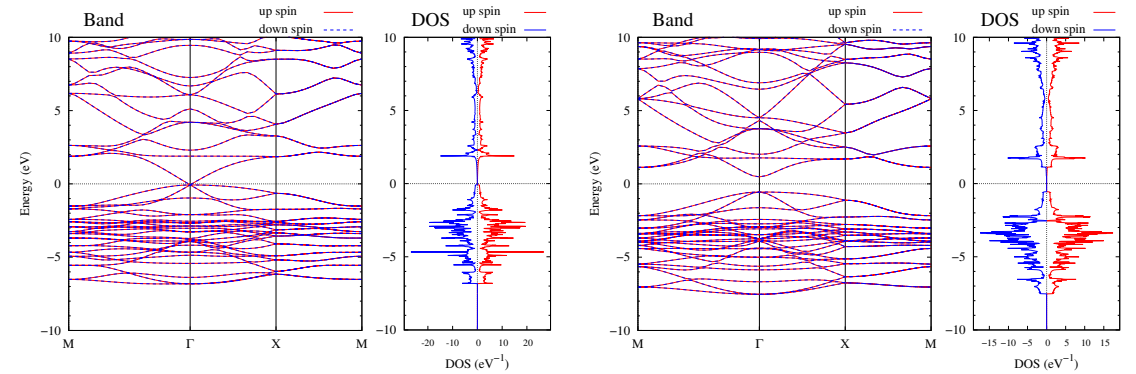

(a) θ-Au_2S (b) η-Au_2S

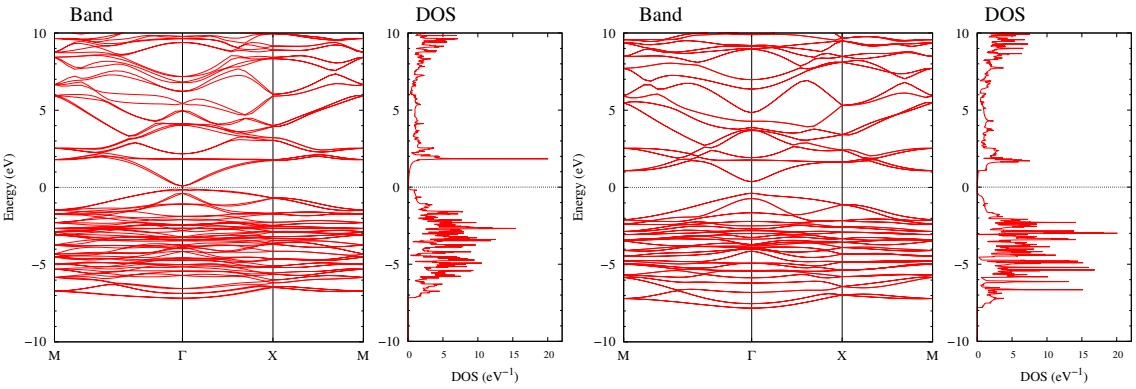

(c) θ-Au_2S (rel) (d) η-Au_2S (rel)

FIG. S1: Electronic band structures and DOSs of Au_2S monolayers based on non-relativistic DFT (a,b) and that with spin-orbit coupling term (c,d). Non-relativistic DFT calculations also include relativistic effect in the pseudopotentials. The y axis is taken so that the Fermi energy is zero.

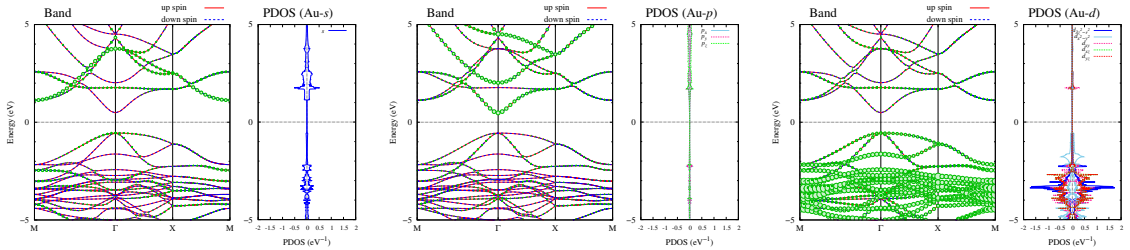

(a) Au-s (b) Au-p (c) Au-d

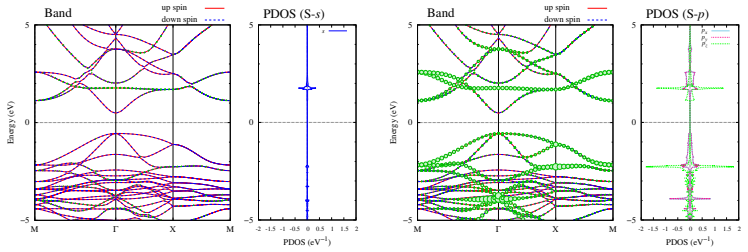

(d) S-s (e) S-p

FIG. S2: Weight of the electronic band and partial DOS of Au and S atoms of *buckled-η*-Au_2S monolayers. The weight is projected on s, p and d type functions.

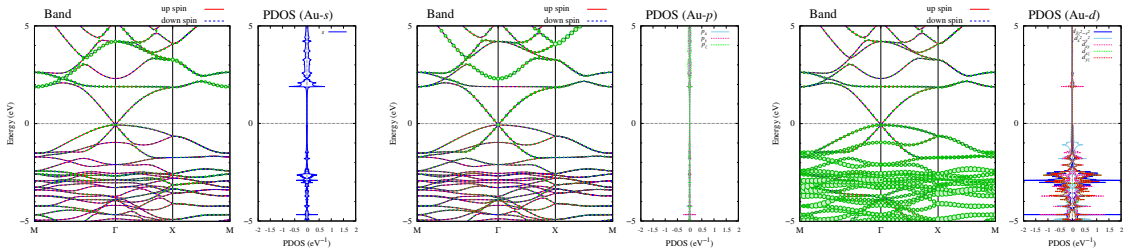

(a) Au-s (b) Au-p (c) Au-d

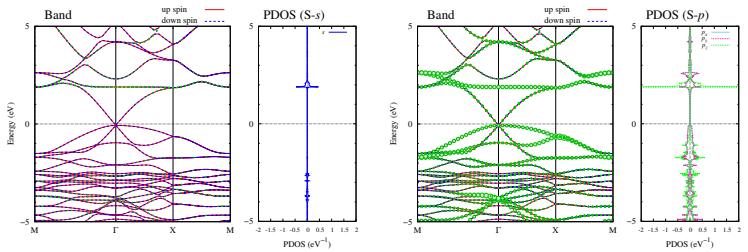

(d) S-s (e) S-p

FIG. S3: Weight of the electronic band and partial DOS of Au and S atoms of *buckled-θ*-Au_2S monolayers. The weight is projected on s, p and d type functions.

TABLE S3: Function types for each band.

Band	Function Types
CB2	Au-s,d, S-p_z
CB1	Au-p_x,p_y
VB1	Au-d, S-p_x,p_y
VB2	Au-d, S-p_x,p_y

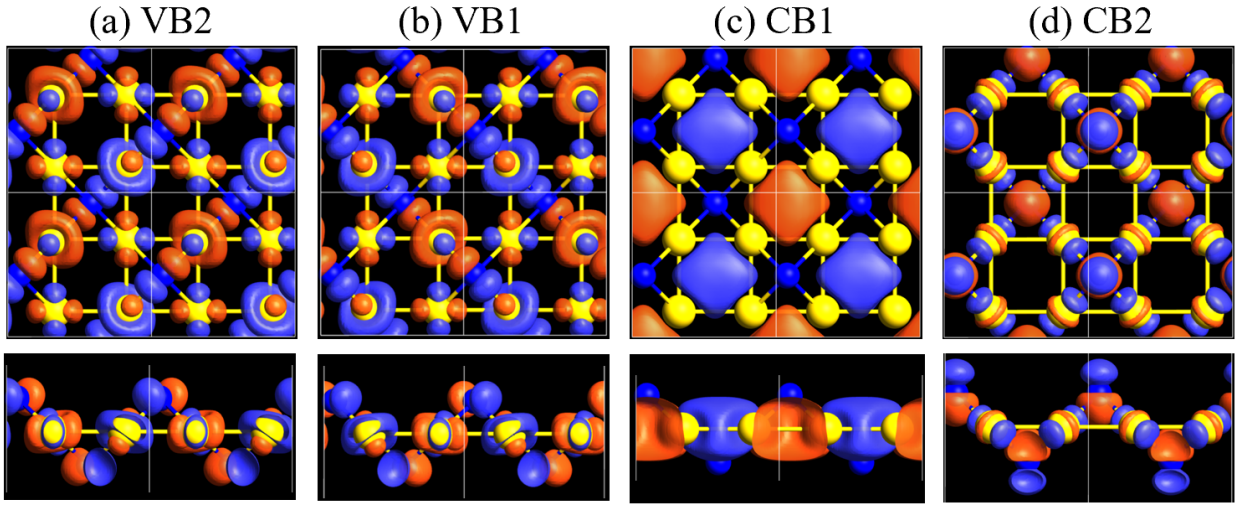

FIG. S4: Molecular orbitals (MO) of VB2, VB1, CV1, and CV2 of *buckled-η*-Au_2S monolayers at Γ point. The threshold value of isosurfaces of the MOs is taken as 0.04 a.u. .

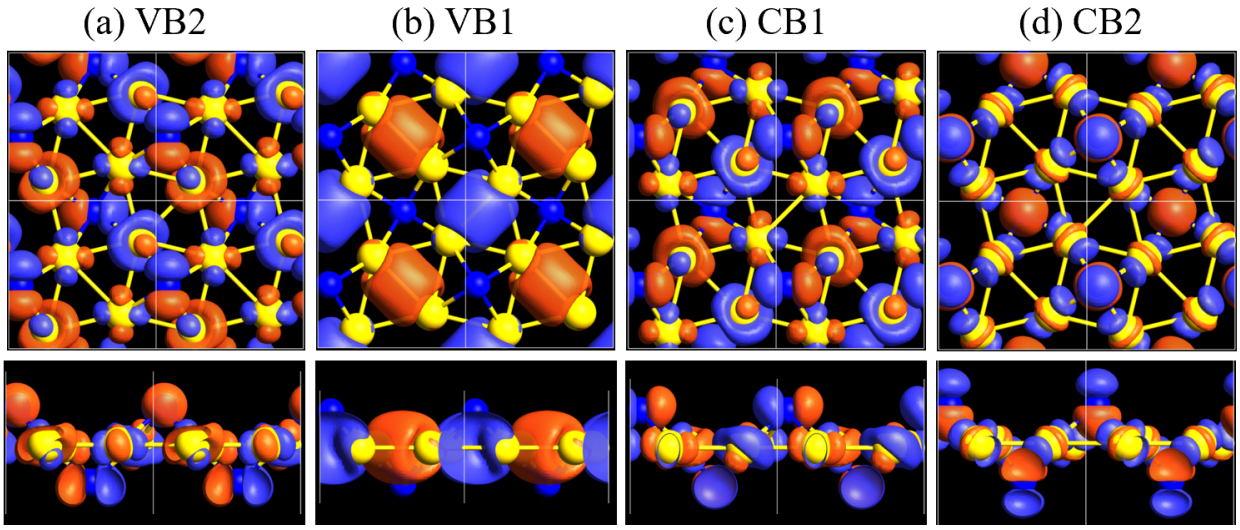

FIG. S5: Molecular orbitals (MO) of VB2, VB1, CV1, and CV2 of *buckled-θ*-Au_2S monolayers at Γ point. The threshold value of isosurfaces of the MOs is taken as 0.04 a.u. . The CB1, VB1 and VB2 are almost degenerate at Γ point.

B. Au_2X monolayers

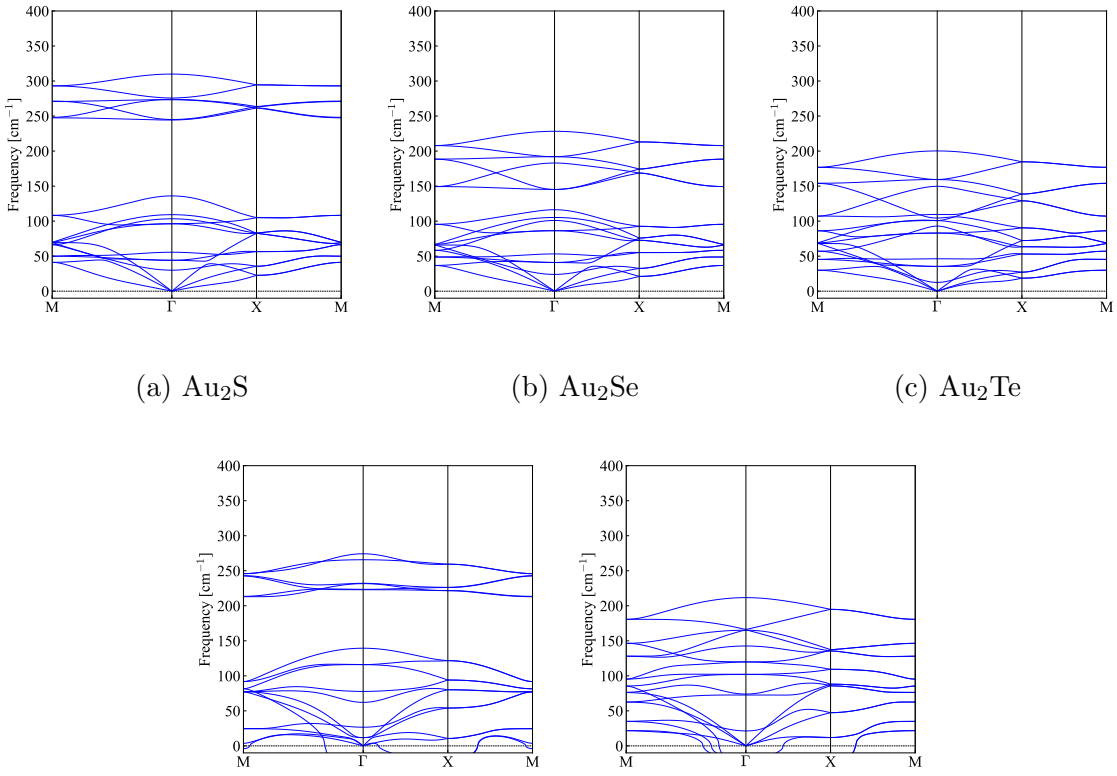

(a) Au_2S (b) Au_2Se (c) Au_2Te

(d) Au_2Si (e) Au_2Ge

FIG. S6: Phonon band of *buckled-η*-Au_2X (X=S, Se, Te, Si, Ge). The phonon band is calculated based on the partition method. We applied the r^{-4} weight for atoms in the region $0.4r_{\text{inner}} < r < r_{\text{outer}}$ to obtain proper results.

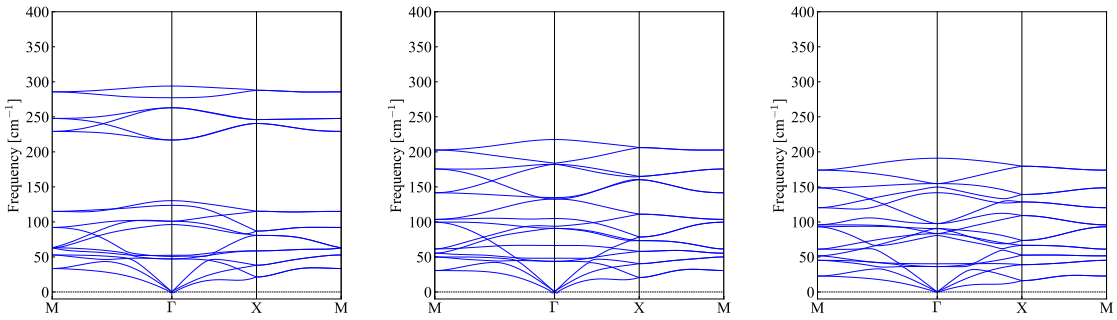

(a) Au_2S (b) Au_2Se (c) Au_2Te

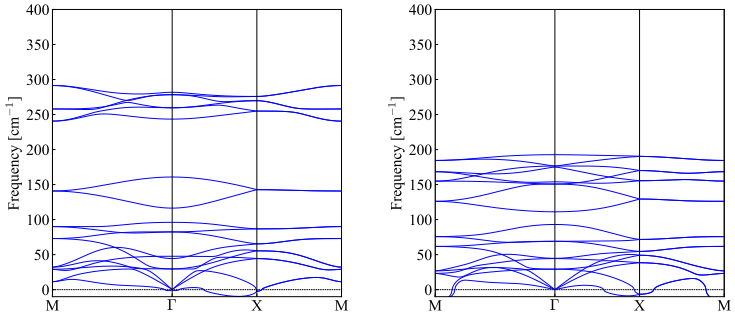

(d) Au_2Si (e) Au_2Ge

FIG. S7: Phonon band of *buckled-θ*-Au_2X (X=S, Se, Te, Si, Ge). The phonon band is calculated based on the partition method. We applied the r^{-4} weight for atoms in the region $0.4r_{\text{inner}} < r < r_{\text{outer}}$ to obtain proper results. For Au_2S and Au_2Se, we applied the r^{-3} weight to obtain proper results.

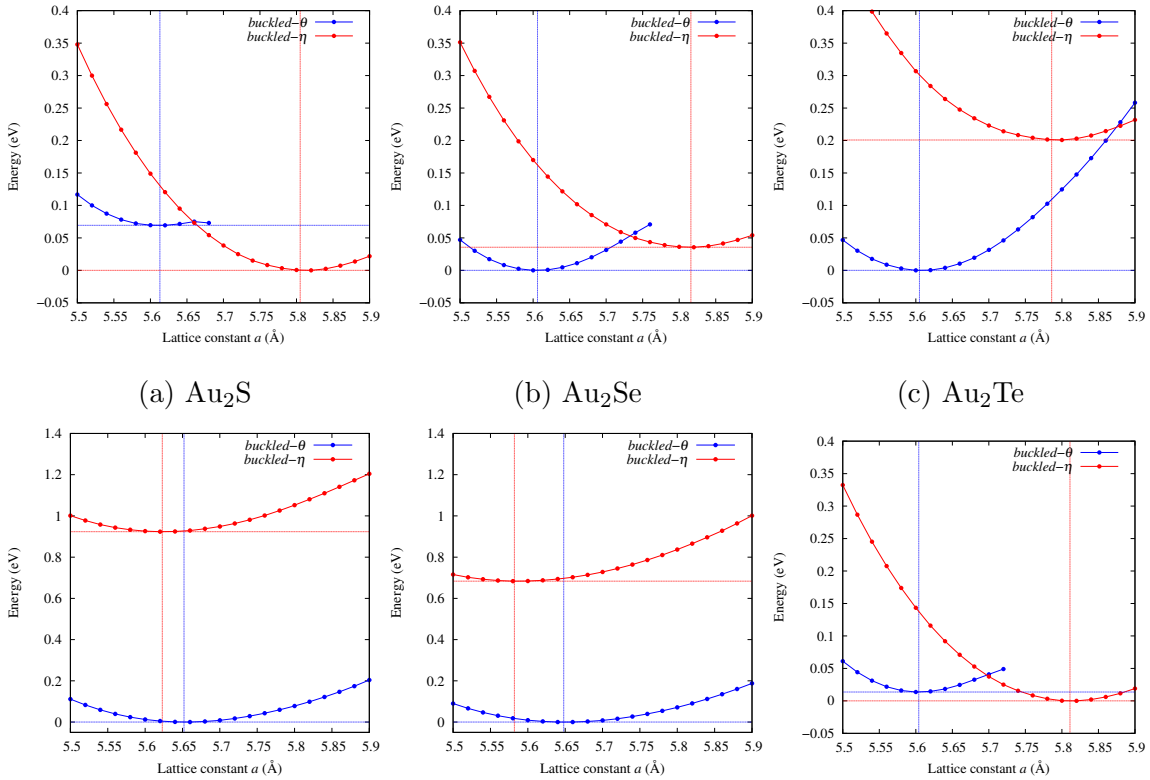

(a) Au_2S (b) Au_2Se (c) Au_2Te

(d) Au_2Si (e) Au_2Ge (f) Au_4SSe

FIG. S8: Energy curve of *buckled-η-* and *buckled-θ-* Au_2X (X=S, Se, Te, Si, Ge) and Au_4SSe monolayers. The red (blue) line represents the energy curve of η-phase (θ-phase).

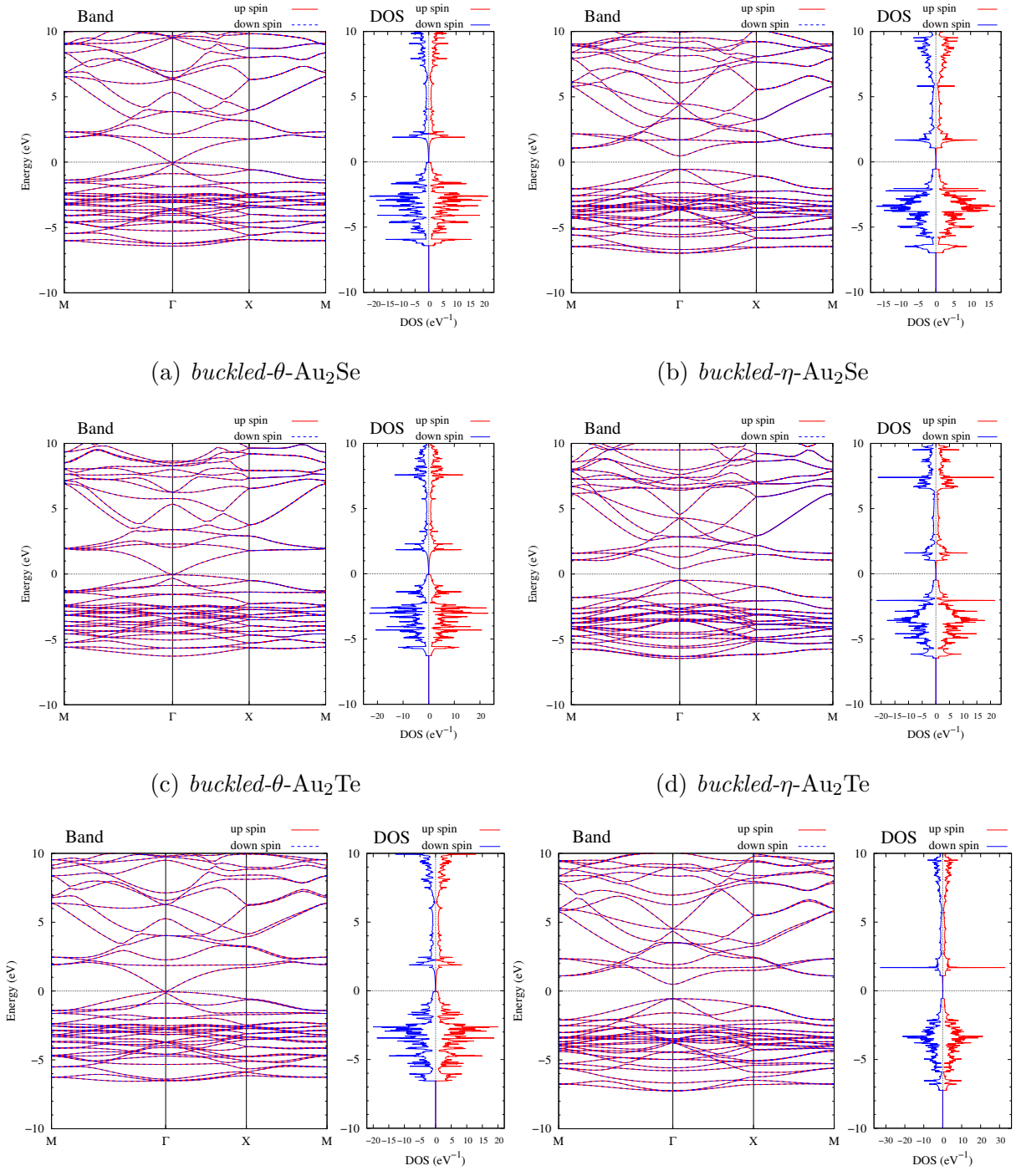

(a) *buckled-θ*-Au_2Se (b) *buckled-η*-Au_2Se

(c) *buckled-θ*-Au_2Te (d) *buckled-η*-Au_2Te

(e) *buckled-θ*-Au_4SSe (f) *buckled-η*-Au_4SSe

FIG. S9: Electronic band and DOS of Au_2X (X=Se, Te) and Au_4SSe monolayers.

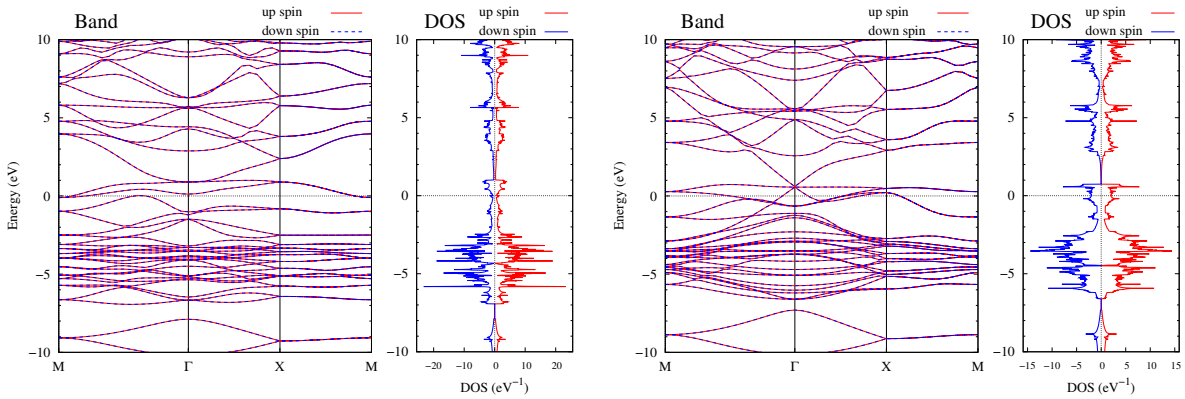

(a) *buckled-θ*-Au_2Si (b) *buckled-η*-Au_2Si

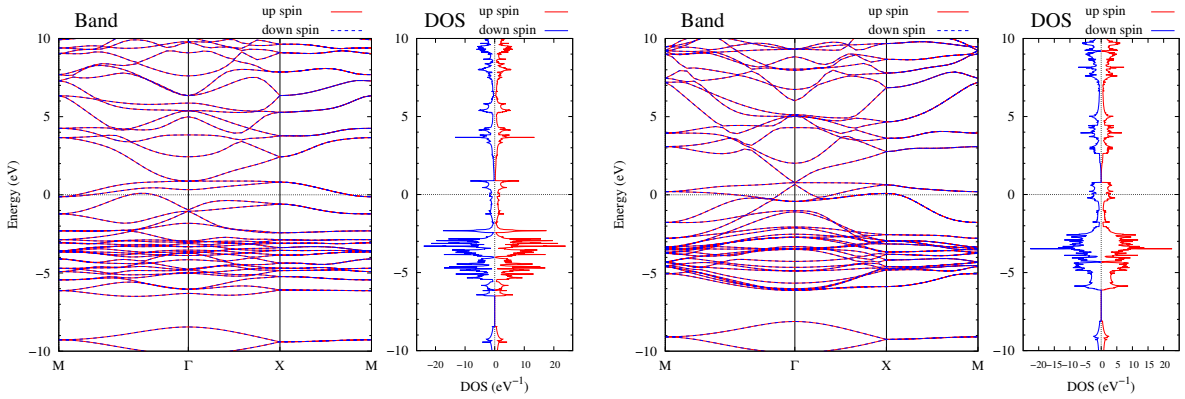

(c) *buckled-θ*-Au_2Ge (d) *buckled-η*-Au_2Ge

FIG. S10: Electronic band and DOS of Au_2X (X=Si, Ge) monolayers.

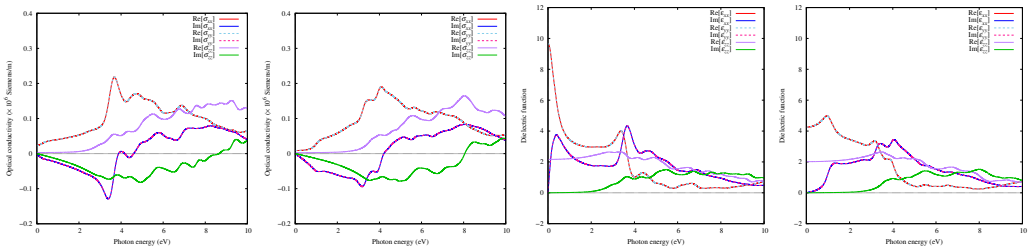

(a) θ-Au_2S (b) η-Au_2S (c) θ-Au_2S (d) η-Au_2S

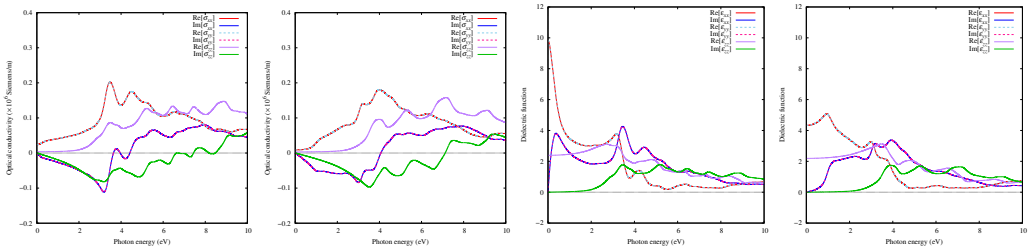

(e) θ-Au_2Se (f) η-Au_2Se (g) θ-Au_2Se (h) η-Au_2Se

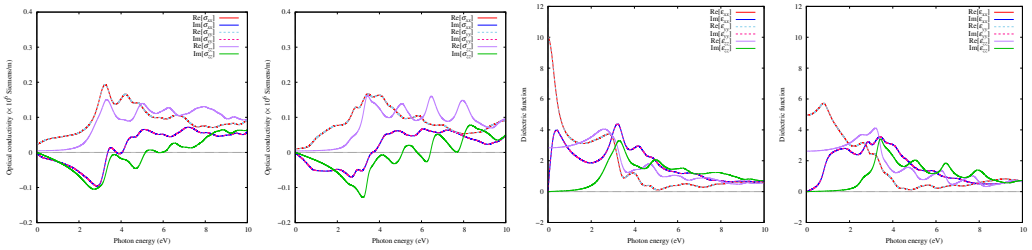

(i) θ-Au_2Te (j) η-Au_2Te (k) θ-Au_2Te (l) η-Au_2Te

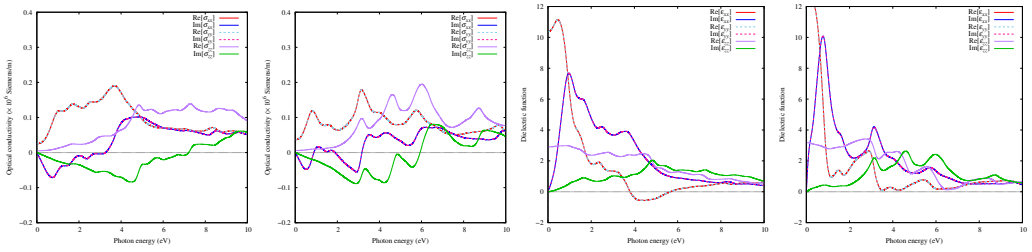

(m) θ-Au_2Si (n) η-Au_2Si (o) θ-Au_2Si (p) η-Au_2Si

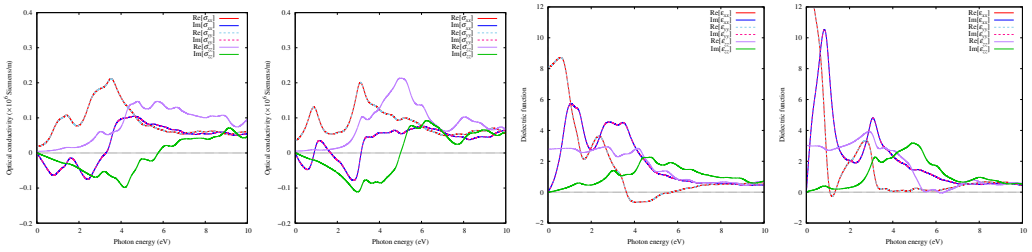

(q) θ-Au_2Ge (r) η-Au_2Ge (s) θ-Au_2Ge (t) η-Au_2Ge

FIG. S11: Optical conductivities (left two columns) and dielectric functions (right two columns) of Au_2X (X=S, Se, Te, Si, Ge) monolayers.